

# Hartmann wave-front scanner

Vincent Laude, Ségolène Olivier, Carine Dirson, and Jean-Pierre Huignard

Laboratoire Central de Recherches, Thomson-CSF, F-91404 Orsay Cedex, France

Received July 29, 1999

A wave-front sensor is described that uses a programmable moving aperture to scan an incoming wave front. The position of the diffraction spot is recorded behind an objective lens with a two-dimensional sensor and gives an estimate of the local slope at the aperture position. Then the wave front is reconstructed by processing of the slope data. The device is basically a programmable Hartmann wave-front sensor. Compared with a microlens Shack–Hartmann wave-front sensor, its much longer focal length provides higher resolution, although real-time operation is lost. A practical implementation of the new scanner with a liquid-crystal television as the programmable aperture is presented. © 1999 Optical Society of America

OCIS codes: 010.7350, 120.5050, 230.6120.

Interest in wave-front sensing has been driven mainly by adaptive optics.<sup>1</sup> In adaptive optics, the wave front is a function of time, and the processing speed of the wave-front sensor is of utmost importance. A closely related application is the sensing of laser wave fronts, for which the compensation of static or dynamic aberrations is required for attainment of diffraction-limited beams. A third type of application of wave-front sensing is the noncontact testing of optical components, in which case only static aberrations have to be measured but the required precision is generally more stringent than for adaptive optics or laser beam sensing. Each of these various applications has its particular characteristics and demands, and no single wave-front sensor is clearly better. Instead, many solutions have been proposed, most of which can be classified into one of three types. Phase-difference sensors, e.g., Michelson, Twyman–Green, and Fizeau interferometers, provide direct measurement of the wave-front phase at some wavelength compared to some reference wave-front phase. They are widely used for optical testing but do not lend themselves easily to adaptive optics or laser beam sensing. The Shack–Hartmann sensor,<sup>2</sup> which is widely used for adaptive optics, and the three-wave lateral shearing interferometer<sup>3</sup> are typical of wave-front sensors that measure the local slopes of the wave front. A third type, curvature sensing devices, was also proposed.<sup>4</sup>

The wave-front sensor presented in this Letter is of the second type.<sup>1</sup> Its principle is that the light going through a small hole in an opaque mask superimposed upon the wave front will form a diffraction pattern in the focal plane of an observation lens that is shifted angularly according to the local slope of the wave front. This gives essentially a sample of the derivative of the wave front at the aperture position. A major improvement in the Hartmann test is the use of a lenslet array as a replacement of the hole plate in the Shack–Hartmann sensor.

The original Hartmann principle is often employed for inspection of optical components, but a mask with holes provides data that are not always easily processed with a wave-front reconstruction algorithm. However, this shortcoming can easily be overcome<sup>5,6</sup>

if the mask is made programmable, i.e., if the aperture can be moved at will across the wave front and the position of the diffraction pattern at a distance  $d$  behind a lens of focal length  $f$  is measured and memorized throughout this scanning process, as depicted in Fig. 1. If  $x'$  is the measured displacement, then

$$\frac{\partial W(x, y)}{\partial x} = \frac{x'}{d} - \left( \frac{1}{f} - \frac{1}{d} \right) x, \quad (1)$$

and a similar equation holds for  $\partial W/\partial y$ . From these data, the wave front can be estimated in a modal or zonal way, much as with a Shack–Hartmann sensor. Unlike the former, the wave-front scanner assumes a static wave front, but its sampling characteristics can be programmed almost arbitrarily. Apart from its sequential nature, this wave-front scanner differs from the Shack–Hartmann sensor for two main reasons: First, the focal length is not necessarily in the usual range of lenslet arrays, i.e., a few centimeters, but can be much longer, say, 1 m. Hence the angular sensitivity should be much higher with the same detector size. Second, the whole surface of the two-dimensional detector is used for every single measurement, whereas in the Shack–Hartmann case only

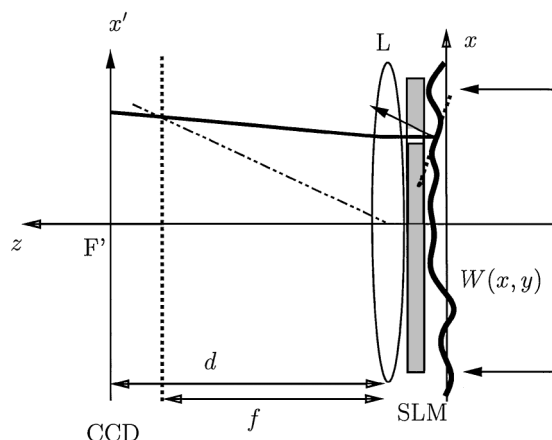


Fig. 1. Schematic of the wave-front scanner: SLM, spatial light modulator.

a subregion of the detector is attributed to each lenslet aperture. Hence one will use a much larger number of pixels to estimate the position of the diffraction spot. It is customary with Shack–Hartmann sensors that the diffraction spot is sampled on a few pixels only, with the consequence that accurate calibration of the pixels' sensitivity is a prerequisite for accuracy in subpixel position estimation. Because many pixels can be used for the same purpose in a wave-front scanner, the quality requirement for the two-dimensional detector can be relaxed. The angular sensitivity can be estimated by

$$\delta\theta = (1/q)(p/d), \quad (2)$$

where  $p$  is the CCD pixel size,  $d$  is the observation distance, and  $q$  is the fractional degree of subpixel position estimation; e.g.,  $q = 10$  if this estimation is one tenth of a CCD pixel. The angular dynamic range is given by

$$\Delta\theta = M(p/d), \quad (3)$$

where  $M$  is the number of CCD pixels. Note that, in the case of the Shack–Hartmann sensor,  $M$  is usually divided by the number of subapertures. The ratio  $\Delta\theta/\delta\theta = qM$  is independent of the focal length used, which results in a simple trade-off between dynamic range and resolution of the wave-front scanner.

We have constructed a wave-front scanner based on a liquid-crystal television (LCTV) between two polarizers used as the programmable aperture. The LCTV that we used<sup>7</sup> has  $640 \times 480$  pixels, with a pixel pitch of  $40 \mu\text{m}$  and a fill factor of  $\sim 0.56$ . The total surface that can be scanned is then  $2.56 \text{ cm}$  by  $1.92 \text{ cm}$ . Pixels are grouped to define the sampling aperture, whose typical size is  $200 \mu\text{m}$  to  $1 \text{ mm}$ . The shape of the aperture is usually rectangular but could be set arbitrarily. The number of sampling points on the wave front can be varied typically from 10 to 100 in each direction. This versatility has a direct influence on the total sampling time; hence one can perform a first scan with low resolution to verify the setup before a high-precision final scan is performed. A frame grabber with separate acquisition and display memories is used to control both the LCTV and a CCD camera. The diffraction spot is observed near the focal plane of an objective lens. The focal lengths that we used were 200, 300, 600, and 800 mm, depending on the wave-front characteristics. Shorter or longer focal lengths could obviously be used as well. The CCD camera used has  $11\text{-}\mu\text{m}$  square pixels, and the acquired image has  $640 \times 480$  pixels.

We used the classic centroid method to estimate the center of the diffraction spots. A typical diffraction spot obtained with our setup is shown in Fig. 2. The centroid calculation was performed inside a window of  $100 \times 100$  CCD pixels. The repeatability of the centroid estimation was found to be one tenth of a CCD pixel, i.e.,  $\delta\theta = 1.4 \mu\text{rad}$  for the  $f = 800 \text{ mm}$  lens. However, the practical resolution, as limited by opti-

cal noise in the setup, was found to be of the order of  $5 \mu\text{rad}$  rms with the same focal length, which could probably be reduced further if the optical quality of the components in the setup were improved. The angular dynamic range  $\Delta\theta$  is 8.8 by 6.6 mrad.

Many wave-front reconstruction algorithms from the slopes have been proposed.<sup>1</sup> Zonal algorithms aim at estimating a sampled version of the wave front, with the sample points generally located at the same position as the slope points. Zonal reconstruction methods can be either direct or iterative.<sup>8</sup> Modal algorithms assume that the wave front can be described as a combination of given parametric functions, or modes. Orthogonal polynomials are often used for this purpose because they provide an exact expansion basis. However, this expansion is in practice truncated to a given order, with the result that the estimation can be biased if high-frequency details in the actual wave front are not adequately described by the polynomials retained. We have chosen to use a modal reconstruction method based on Southwell's algorithm.<sup>9</sup> The orthogonal polynomials used are the 48 first Legendre polynomials,<sup>9</sup> because the scanning aperture defined by the spatial light modulator is rectangular. The wave front is expanded as

$$W(x, y) = \sum_{m=0}^6 \sum_{n=0}^6 a(m, n)P_m(x)P_n(y). \quad (4)$$

The piston term ( $m = n = 0$ ) is excluded from expansion (4) because a piston cannot be sensed by the Hartmann test. The unknown coefficients  $a(m, n)$  are obtained by minimization of a least-squares criterion that measures the distance between the slope measurements and the model of Eq. (4). The solution of this problem is well known<sup>9</sup> and is not repeated here.

Figure 3(a) shows the experimental slopes that were obtained with a progressive ophthalmic lens as the sample. This object was chosen for its high dynamic range and lack of revolution symmetry, to show that rather complicated, although smooth, wave fronts can be sensed with high accuracy. The focal length used is 200 mm, with the rms acquisition noise estimated to be  $\sim 15 \mu\text{rad}$ . Acquisition noise cannot be seen in Fig. 3(a) because of the steep slopes observed;  $29 \times 22$  slope measurements are produced with a spacing of  $800 \mu\text{m} \times 800 \mu\text{m}$ . The total scanning time is of the order of 2 min and is limited by the duration of three steps involved for each sample point, i.e., generation of the aperture pattern onto the spatial light modulator, acquisition of a video frame, and centroid calculation. The duration of each of these steps could probably be reduced by 1–2 orders of magnitude by use

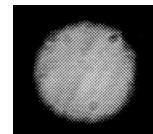


Fig. 2. Typical diffraction spot.

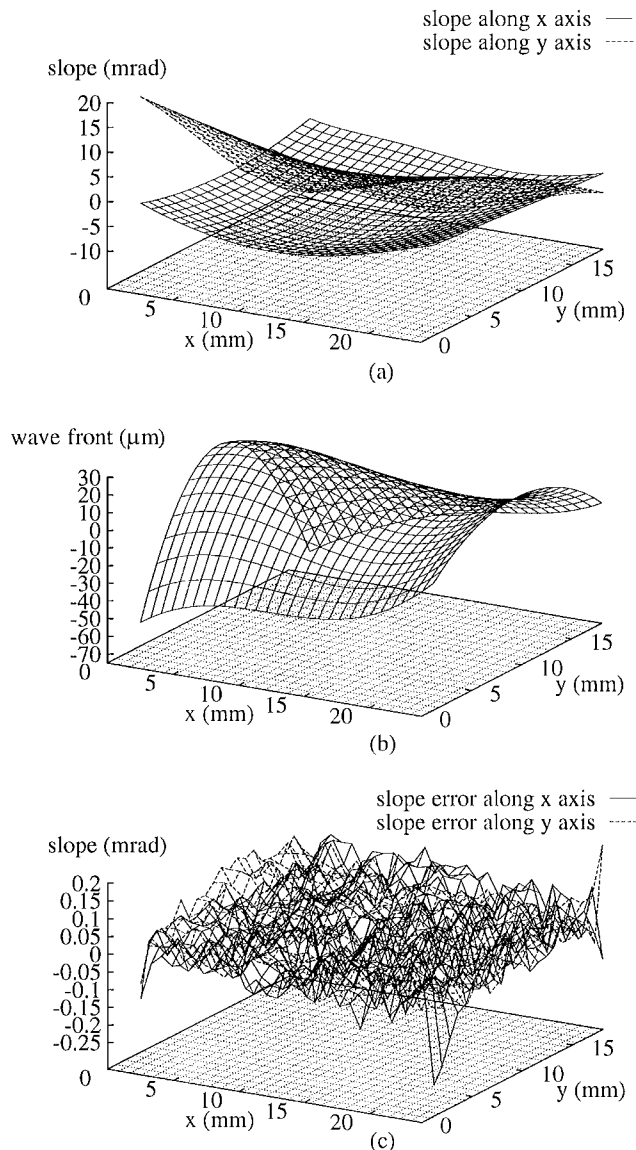


Fig. 3. Reconstruction of the wave front after an ophthalmic progressive lens: (a) experimental slopes, (b) reconstructed wave front, (c) residual reconstruction error.

of optimized hardware. Figure 3(b) shows the reconstructed wave front from which we have removed tilt aberration, because tilt can result from the positioning of the tested object and is generally not part of the object aberration. The reconstructed wave front shows mainly a variation of the  $y$  curvature along the  $x$  axis, in intuitive agreement with the purpose of a progressive ophthalmic lens, i.e., a vertically varying fo-

cal length. Figure 3(c) shows the difference between the reconstructed slopes, as obtained by differentiation of Eq. (4), and the experimental slopes. This is a quantitative indication of the quality of the reconstruction. The result is a zero-mean white-looking noise with standard deviations of 42 and 35  $\mu\text{rad}$  along the  $x$  and  $y$  axes, respectively. Compared with the estimated 15- $\mu\text{rad}$  rms acquisition noise, it can be concluded that most of the reconstruction error arises from acquisition noise rather than from the reconstruction procedure itself. Expressed differently, the truncation of the modal description of Eq. (4) does not introduce a significant bias over the noise level for the tested wave front.

Because of the sequential nature of the wave-front scanner, it should be inapplicable to problems that require real-time operation, such as adaptive optics. However, whenever accuracy, programmability, or dynamic range is a key parameter and the wave front is static, the wave-front scanner could be a useful alternative to existing wave-front sensors. Examples of such applications are optical testing and laser beam analysis.

The principle of a scanning wave-front sensor has been described. The device is achromatic, offers a high accuracy together with a large dynamic range, and is free from the ambiguities between sampling points that affect Shack-Hartmann sensors. No critical or high-cost elements are required, especially for detection. The sampling geometry, and especially the size and number of sampling points, can be programmed easily. The drawback of the sequential nature of the sensor is that real-time operation is not possible. A practical implementation based on a LCTV was presented, and the experimental reconstruction of the wave front from a progressive ophthalmic lens was discussed, showing both resolution and dynamic range.

V. Laude's e-mail address is laude@lcr.thomson-csf.com.

## References

1. R. K. Tyson, *Principles of Adaptive Optics* (Academic, San Diego, Calif., 1991).
2. R. V. Shack and B. C. Platt, *J. Opt. Soc. Am.* **61**, 656 (1971).
3. J. Primot, *Appl. Opt.* **32**, 771 (1993).
4. F. Roddier, *Appl. Opt.* **27**, 1223 (1988).
5. G. Hausler and G. Schneider, *Appl. Opt.* **27**, 5160 (1988).
6. C. Castellini, F. Francini, and B. Tiribilli, *Appl. Opt.* **33**, 4120 (1994).
7. V. Laude, *Opt. Commun.* **153**, 134 (1998).
8. F. Roddier and C. Roddier, *Appl. Opt.* **30**, 1325 (1991).
9. W. H. Southwell, *J. Opt. Soc. Am.* **70**, 998 (1980).